

## THE EFFECT OF INDUCED MAGNETIC ANISOTROPY ON THE HYSTERESIS PARAMETER OF NANO BARIUM STRONTIUM HEXAFERRITE PREPARED BY MECHANICAL ALLOYING AND SONICATION

Novizal<sup>1\*</sup>, Azwar Manaf<sup>2</sup>, Musfirah Cahya Fajrah<sup>1</sup>

<sup>1</sup> *Department of Physics, Faculty of Mathematics and Sciences, Institute Sciences and Technology National, Jakarta 12640, Indonesia*

<sup>2</sup> *Department of Physics, Faculty of Mathematics and Sciences, Universitas Indonesia, Kampus UI Depok, Depok 16424, Indonesia*

(Received: December 2015 / Revised: January 2016 / Accepted: February 2016)

### ABSTRACT

In this research, analysis of the magnetic properties of the nanoscale ferromagnetic material barium strontium hexaferrite with the composition of  $Ba_{(0.7)}Sr_{(0.3)}O_6(Fe_2O_3)$  or written as  $B_7S_3HF$  is conducted. The material was prepared by the ball mill method, followed by reducing the particle sizes of the material to reach a result in nanometers with a high pressure ultrasonic for 12 hours. In the compacting process, a parameter was given from the outside of the 50 mT magnetic field to determine the cause of the anisotropy phenomenon of the material. To identify the phase of material, changes in the magnetic properties and measurement of the Particle Size of the  $B_7S_3HF$  material were taken. The equipment used was X-Ray Diffraction (XRD), Permagraph (an automatic computer-controlled measuring system) and Particle Size Analyzer (PSA). The results of XRD were seen in their influence against the Buffered Hydrofluoric (BHF) acid, which were caused by the effects of the Strontium (Sr) substitution and by increasing the size of the material volume. Changes in the magnetic properties of the  $B_7S_3HF$  material, due to an induced magnetic field from the outside, were caused in contrast with the remanent value ranging from 0.18 T up to 0.249 T, respectively. This process did not occur, since the coersivity value was fixed at  $275.54 \text{ kAm}^{-1}$ . Changes in the value of the remanent material rose by 0.069 T or (6.9%). This phenomenon shows the anisotropy influence in the  $B_7S_3HF$  material in an external magnetic induction of 50 mT. The results of the ultrasonic measurements were performed using Particle Size Analyzer (PSA) equipment, which gained a 43.5 nm particle size.

**Keywords:** Magnetic induction; Mechanical alloying; Remanent coercivity; Sonication

### 1. INTRODUCTION

Barium Strontium hexaferrite  $Ba_{(0.7)}Sr_{(0.3)}Fe_{12}O_{19}$  or ( $B_7S_3HF$ ) is well known and it has gained a lot of attention in recent years as one of the candidates for high density magnetic recording media because the physical properties of the material itself is unique. The physical properties include a high Curie temperature, large magnetic anisotropy, good magnetization, excellent chemical stability, and a large Kerr and Faraday rotation (Rajath et al., 2008; Sharma et al., 2006). However, the most important part of the research is to make  $Ba_{(0.7)}Sr_{(0.3)}Fe_{12}O_{19}$  with stable coercivity, perpendicular-anisotropy and small grain size for high density magnetic recording media. Many ways are used to enhance the magnetic properties of  $Ba_{(0.7)}Sr_{(0.3)}Fe_{12}O_{19}$

---

\*Corresponding author's email: novizal@istn.ac.id, Tel. +62-8119693889  
Permalink/DOI: <http://dx.doi.org/10.14716/ijtech.v7i3.2932>

with stable coercivity, perpendicular-anisotropy and small grain size for high density magnetic recording media. Many ways are used to enhance the magnetic properties of  $\text{Ba}_{(0.7)}\text{Sr}_{(0.3)}\text{Fe}_{12}\text{O}_{19}$ . One of these methods is divalent ion substitution, for example, using Sr ions in the ion Ba (Rangel et al., 2006; Wang et al., 2005; Niu et al., 2006). This method provides a limited improvement in the magnetic properties of  $\text{Ba}_{(0.7)}\text{Sr}_{(0.3)}\text{Fe}_{12}\text{O}_{19}$  because the particles produced have a large size. One promising method to enhance the magnetic properties of  $\text{Ba}_{(0.7)}\text{Sr}_{(0.3)}\text{Fe}_{12}\text{O}_{19}$  is preparing materials of nano-particles which, as the particle size decreases, the magnetic coercivity decreases (Krishnaveni et al., 2006). The purpose of this research is to improve the magnetic properties of  $\text{Ba}_{(0.7)}\text{Sr}_{(0.3)}\text{Fe}_{12}\text{O}_{19}$  by providing magnetic induction from the outside during the compaction process of the sample nanoparticles.

## 2. EXPERIMENTAL SETUP

This study uses a mechanical alloying method with a planetary ball mill. This process begins with the contact particles and then follows with the forming of layers which occur due to the collision that is called the cold welding process. After reaching a homogeneous phase, the process is followed by fracturing (embrittlement), which results in particle size reduction in subsequent collisions. In preparation for samples that are formed of solids (bulk), the sample surface is smoothed to reduce the effects of surface roughness and a radial shift (radial displacement) occurs. Powder samples were prepared by means of top loading, using a sample holder formed of acrylic with a depth of 2 mm to remove the effect of transmission and preferred orientation.

Characterization by XRD was accomplished using a Philips PW3710 Diffractometer with an anode Co, 1/40 divergence slit, receiving slit 1/5 and calibrated Si-standard on  $33.124^\circ$  angle and by using the software menu on the treatment pattern with a Phillips Automated Powder Diffractometer (APD). Data is collected on a 20-100 degree angle with 0:02 step-scan and scan time of 1 second which produces 4000 Data for ~1 hour. The particle size distribution is characterized by a Malvern Zetasizer Ver. 6:20, Particle Size Analyzer (PSA) with the ability to 20 nm. For samples, such as a BHF magnetic, the attractive force between the magnetic particles is very strong and it needs to be separated by the use of high power ultrasonic and the addition of a surfactant to prevent agglomeration, so that the data produced are related to a true particle size.

The morphology of the samples was characterized by a Scanning Electron Microscope (SEM), Type FEI-F50, which is capable of achieving magnifications up to 200,000 $\times$ . The magnetic characterization of the samples is done by using a Permagraph EP.3 magnetometer with a maximum induction field strength of 92 mm poles (1700 kA/m) and a 2 mm air gap (21.5 kOe). Variables were entered in the form of density data. Data acquisition software is used with a density meter to generate data that does not depend on the volume or size of the sample. Materials used for the manufacture of the material are composed of base materials in powder form, namely barium carbonate ( $\text{BaCO}_3$ ), iron oxide powder ( $\text{Fe}_2\text{O}_3$ ), and strontium carbonate ( $\text{SrCO}_3$ ), which are used to make the material  $\text{B}_7\text{S}_3\text{HF}$  (Barium Strontium hexaferrite). The composition for  $\text{Ba}_{(0.7)}\text{Sr}_{(0.3)}\text{Fe}_{12}\text{O}_{19}$  is encoded with  $\text{B}_7\text{S}_3\text{HF}$  powder nano-particles and is prepared by a ball mill and a high pressure sonication method (Leyet-Ruiz et al., 2009; Nowosielski et al., 2007).

To obtain a sample in the form of magnetic induction in the bulk, the compacting process is carried out with a pressure of 70 kN with a given external magnetic field of 50 mT. Given the bulk material, the temperature of sintering is  $1100^\circ\text{C}$  to achieve the final results over a period of 4 hours.

### 3. RESULTS AND DISCUSSION

An X-Ray Diffraction of the powder sample is shown in Figure 1a. It is obvious that the prepared sample is manufactured by a mechanical alloying and sonication method. The lattice parameter was found to be about 5,889 Å as shown in Table 1. This was based in reference, which is in good agreement with earlier reports (Arulmurugana et al., 2005; Pandya et al., 1991). Also, from the X-ray pattern, the average crystallite size of the powder sample is found to be about 43 nm (Pankhurst et al., 1996).

This result confirms that the prepared sample has a similar nano-crystallite size. Figure 1b shows the image from the SEM of the powder sample. It is noticeable that the powder sample has nano-sized particles in the range of 43.5 nm, which is in a good agreement with the X-ray measurements.

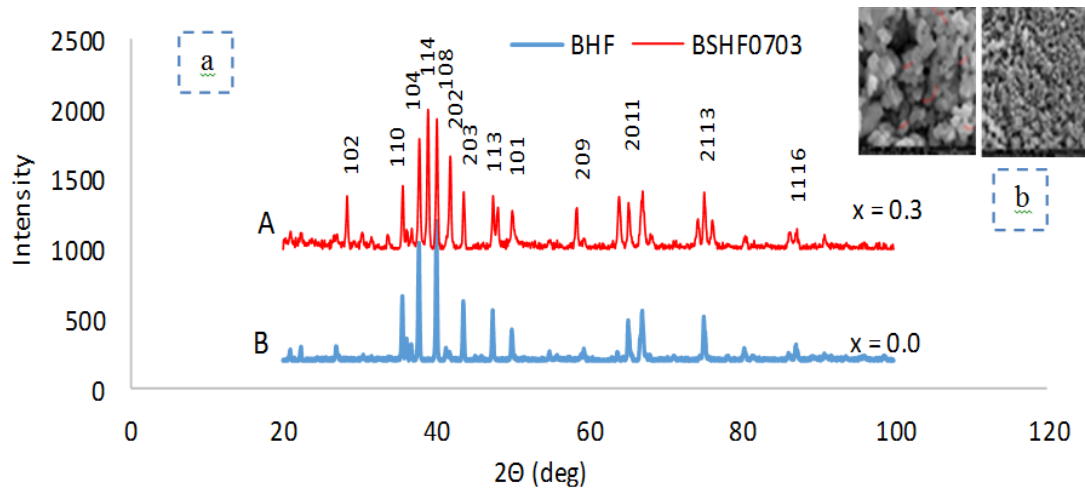


Figure 1 (a) X-ray diffraction pattern; and (b) SEM of  $\text{Ba}_{(0.7)}\text{Sr}_{(0.3)}\text{Fe}_{12}\text{O}_{19}$  nanoparticles

Figures 1a and 1b show the X-ray diffraction to  $\text{B}_7\text{S}_3\text{HF}$ , BHF and (hkl) depicted above is owned by  $\text{B}_7\text{S}_3\text{HF}$  and there are also some belonging to the BHF difference, which is due to the substitution of Sr to BHF. The XRD pattern results shown in Figure 1 indicate the difference in the phase pattern between the BHF phase and  $\text{B}_7\text{S}_3\text{HF}$  as well as with the results of the synthesis of the GSAS to the XRD data of the substituted material  $\text{B}_7\text{S}_3\text{HF}$  with the Sr composition  $x = 0.3$ . The GSAS pattern indicates the occurrence of a material change in intensity and a change on  $\text{B}_7\text{S}_3\text{HF}$  as well. Additionally, the formation of other areas that are not the same as the material BHF, among the emerging field (114), (202), (2011) is apparent. SEM images are the results for samples of  $\text{Ba}_{(0.7)}\text{Sr}_{(0.3)}\text{Fe}_{12}\text{O}_{19}$  that were in sonication for 12 hours. We observed that only the Bragg reflections (in brackets) belonging to the hexagonal phase that appeared, indicated that the samples were single phase materials with references (JCPDS 19-629). The information from the broadened X-ray diffraction lines is normally used to estimate the average size of coherent diffraction domains by using the Scherrer approach (Cao, 2004).

Table 1 Physical information from GSAS results and space group

Material	a (Å)	b (Å)	c (Å)	Crystallite size (nm)	Volume ( $\text{cm}^3$ )	Density ( $\text{g}/\text{cm}^3$ )	Space group
BHF	5,862	5,862	23,109	41	687,725	5.31	P 63/mm c
$\text{B}_7\text{S}_3\text{HF}$	5,889	5,890	23,106	43	694,978	5.35	P 63/mm c

Changes in the value of the lattice parameters  $a(\text{\AA})$ ,  $b(\text{\AA})$ , and  $c(\text{\AA})$ , and additional parameters, such as volume and density, can also influence the magnetic properties of the material. Hysteresis results were obtained from the substitution of Sr on the BHF material into the  $B_7S_3HF$  material. There were visible effects of the substitution of Sr, which changed with the values of remanent and coercivity of the  $B_7S_3HF$  material, as shown in Figure 2. The  $B_7S_3HF$  material has a higher remanent value of BHF. Permagraph results of the BHF and  $B_7S_3HF$  material obtained the remanent value and coersivity of  $B_7S_3HF$  material, which rose by 0.0240 T of the value of the remanent BHF and the coersivity value decreased by 50 kA/m.

From Figure 2 and Table 2, Sr substitution results in the BHF material culminated in the value results of the change in magnetic properties. These are clearly illustrated in the values of saturation, remanence and coercivity change. Table 2 shows the magnetic properties of the BHF and  $B_7S_3HF$  materials, which have a remanent value of 0.1607 T and 0.1804 T respectively, while the value of each coersivity is 322.142 kA/m and 275.540 kA/m, respectively. In Figure 2, the data also show the changes in the value of the saturation, remanence and coercivity picture. The BHF also has greater values than the  $B_7S_3HF$  materials.

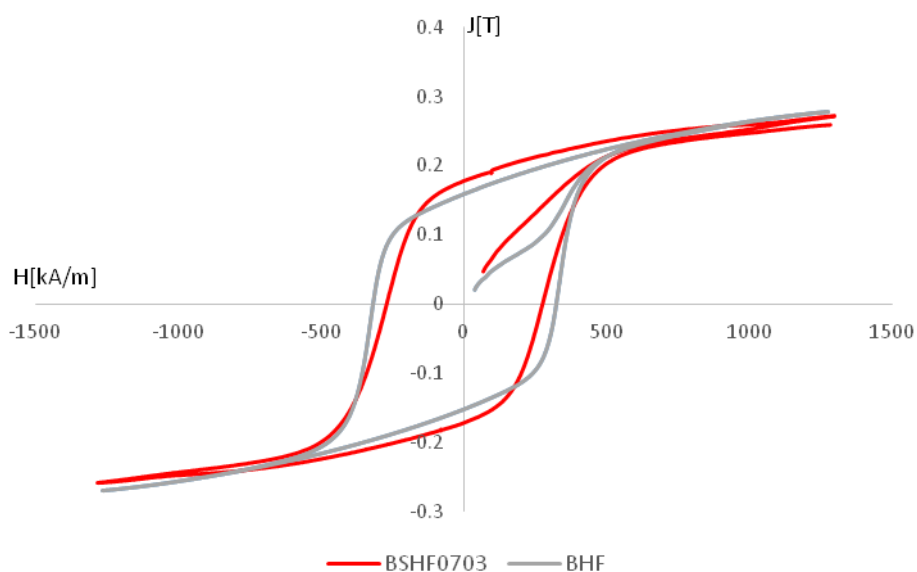


Figure 2 Hysteresis pattern of BHF and  $B_7S_3HF$  materials

Tabel 2 Magnetic properties of BHF and  $B_7S_3HF$  materials

Material	Substitution Sr	Mr	Hcj
BHF	$x = 0.0$	0.1607	322.143
$B_7S_3HF$	$x = 0.3$	0.1804	275.540

The measurement of particle size by using the PSA of the  $B_7S_3HF$  material obtained the particle size and crystal size using XRD and this was synthesized by using the Debey Scherer Theory. With the value of the composition ratio of Ba with Sr being 7:3, the data obtained for the smallest particle size of the  $B_7S_3HF$  material milling results after 80 hours with sintering at  $1100^\circ\text{C}$  is  $14\ \mu\text{m}$  and the size of the crystals of the  $B_7S_3HF$  material is 52 nm, as shown in Table 3 below.

Table 3 List of Particle and Crystal Sizes of the B<sub>7</sub>S<sub>3</sub>HF material milling results after 80 hours, with sintering at 1100°C for 4 hours

Time Milling	Crystal size B <sub>7</sub> S <sub>3</sub> HF, D (nm)	Particle size B <sub>7</sub> S <sub>3</sub> HF, D(μm)
80	52	14
60	58	17
30	70	18
10	110	10

As shown in the chart in Figure 3 below, there are the visible particle sizes and the crystal sizes of the B<sub>7</sub>S<sub>3</sub>HF material. From the calculation of the measurement of the diameter of the particles and crystals, these are not significant enough to change the particle size of the material, so there should be another method to obtain smaller particle sizes approaching then the nano size, using high power ultrasonic (sonication).

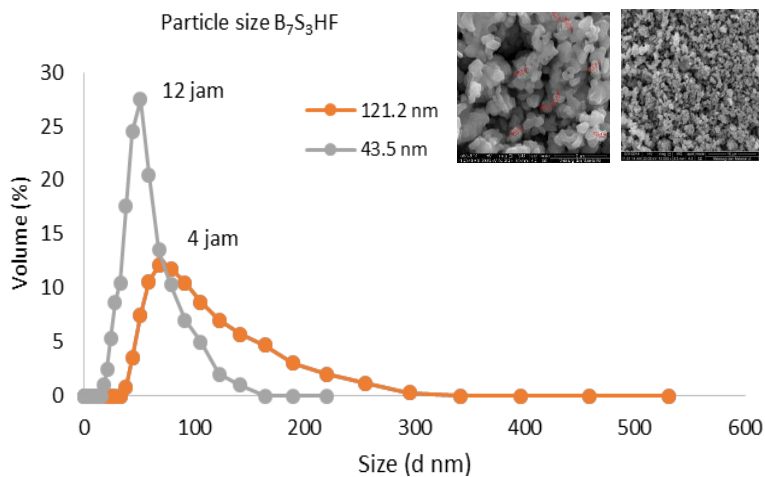


Figure 3 Particle size of B<sub>7</sub>S<sub>3</sub>HF with PSA (nanometer)

Measurement results of the particle size of the B<sub>7</sub>S<sub>3</sub>HF material with PSA sonicated for 4 hours and 12 hours respectively were 121 nm and 43.5 nm as shown in Figure 3. The provision of magnetic induction is shown in Figure 4. The material is in the process of compacting 70 kN, while the magnetic induction is 50 mT.

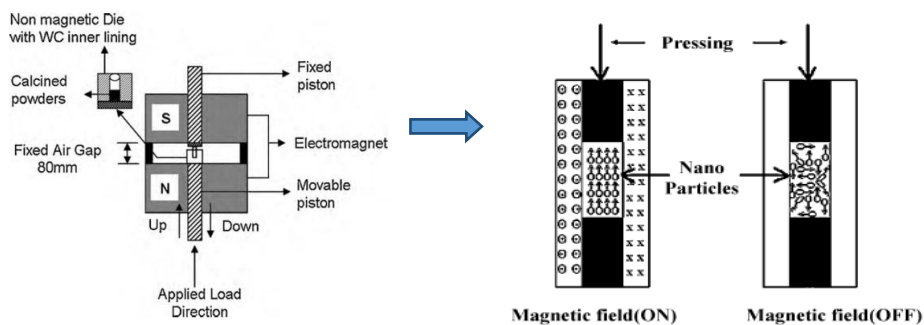


Figure 4 The process of briefing material in the easiest way

The phenomenon that occurs as a result of the provision of the magnetic field induced by 50 mT on the influence of the magnetic field on the material is shown in Figure 5 as indicated in the hysteresis graph of the  $B_7S_3HF$  material. This phenomenon also gives an effect to the magnetic properties of the  $B_7S_3HF$  material (Yang & Chang, 1994).

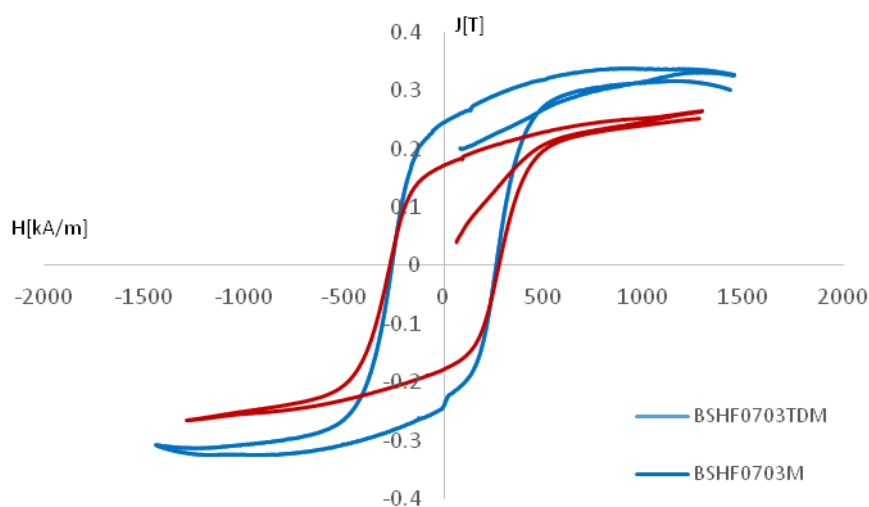


Figure 5 Hysteresis Pattern of the  $B_7S_3HF$  induced magnetic field at 50 mT

The effects of giving the magnetic induction to the  $B_7S_3HF$  material caused changes in the magnetic properties, where the value of remanent increased to 0.069 T, which showed that the remanent for  $B_7S_3HF$  is not within the induction of 0.18 T and the remanent magnetic induction for  $B_7S_3HF$  rose to 0.249 T, and no change occurred in the value of coercivity  $275.540 \text{ kAm}^{-1}$  (Tsuchiya et al., 1992; Coey et al., 1996). The results of the data are shown in Table 4. In this process, the anisotropy phenomenon of the magnetic properties of the  $B_7S_3HF$  material can be seen.

Table 4 The physical properties of the  $B_7S_3HF$  material

Material	$M_r$ (T)	$H_{c_j}$ ( $\text{kAm}^{-1}$ )	Induction magnet
$B_7S_3HF$	0.249	275.540	50 mT
$B_7S_3HF$	0.180	275.540	non

#### 4. CONCLUSION

From all of the data collection processes, the following conclusions can be deduced. Nano Ferromagnetic  $B_7S_3HF$  Materials can be obtained through a mechanical integration process that is accompanied by sintering for the formation of crystalline materials and refinement followed by mechanical and high power ultrasonic (sonification). The average size of the  $Ba_{(0.7)}Sr_{(0.3)}Fe_{12}O_{19}$  or  $B_7S_3HF$  particles reached 43.5 nm, which was obtained after mechanical refining, followed by ultrasonic destruction for 12 hours. The magnetic properties of  $B_7S_3HF$  material is 0.180 T for remanent magnetization and  $275.54 \text{ kA.m}^{-1}$  for the value of coercivity. The remanent magnetization value increased to 0.249 T, due to the effects of anisotropy induced by an external magnetic field of 50 mT without impairment coercivity.

## 5. REFERENCES

- Arulmurugana, R., Jeyadevan, B., Vaidyanathana, G., Sendhilnathan, S., 2005. Effect of Zinc Substitution on Co-Zn and Mn-Zn Ferrite Nano Particles Prepared by Co-precipitation. *Journal of Magnetism and Magnetic Materials*, Volume 288, pp. 470–477
- Cao, C., 2004. *Nano Structures and Nano Materials*. Imperial Collage Press, p. 331
- Coey, J.M., 1996. *Rare Earth Permanent Magnetism*. John Wiley and Sons, New York, p. 220
- Krishnaveni, T., Rajini Kanth, B., Seetha Rama Raju, V., Murthy, S.R., 2006. Fabrication of Multilayer Chip Inductors using Ni-Cu-Zn Ferrites. *Journal of Alloys and Compound*. Volume 414, pp. 282–286
- Leyet-Ruiz, Y., Perez-Rivero, A., Fernandez, M., Perez-Delfin, E., Guerrero, F., Erias, J.A., 2009. Preparation and Characterization of PZT Nano Powder using High Energy Ball Milling. *Revista Cubana De Quimica*, Volume 21, pp. 15–24
- Niu, Z., Wang, Y., Li, S., 2006. Magnetic Properties of Nano Crystalline Co-Ni Ferrite. *Journal of Materials Science*, Volume 41, pp. 5726–5730
- Nowosielski, R., Babilas, R., Dercz, G., Pajak, L., Wrona, J., 2007. Structure and Properties of Barium Ferrite Powders Prepared by Milling and Annealing. *Archives of Materials Science and Engineering*, Volume 28, pp. 735–742
- Pandya, H., Joshi, R., Kulkarni, 1991. Bulk Magnetic Properties of Co-Zn Ferrite Prepared by the Co-precipitation Method. *Journal of Material Science*, Volume 26, pp. 5509–5512
- Pankhurst, Q.A., Thompson, G.R., Sankaranarayanan, V.K., Dikson, D.P.E., 1996. Effect of Ultrafine Particle Size and Crystallinity Breakdown on the Ordered Magnetic State in Barium Ferrite. *Journal of Magnetism and Magnetic Materials*, Volume 155, pp. 104–106
- Rajath, P.C., Mannab, R.S., Banerjee, D., Varma, M.R., Suresh, K.G., Nigamc, A.K., 2008. Magnetic Properties of  $\text{CoFe}_2\text{O}_4$  Synthesized by Solid State, Citrate Precursor and Polymerized Complex Methods: A Comparative Study. *Journal of Alloys and Compound*, Volume 453, pp. 298–303
- Rangel, A.M., Ogasawara, T., Nobrega, M.C., 2006. Investigation of Cobalt-zinc Ferrite Synthesized by Co-precipitation at Different Temperatures: A Relation Between Microstructure and Hysteresis Curve. *Materials Research*, Volume 9(3), pp. 257–262
- Sharma, R.K., Suwalka, O., Lakshmi, N., Venugopalan, K., Banerjee, A., Joy, P.A., 2006. Synthesis of Chromium substituted Nano Particle of Cobalt Zinc-ferrites by Co-precipitation. *Journal of Alloys and Compound*, Volume 59, pp. 3402–3405
- Tsuchiya, T., Yamashiro, H., Sei, T., Inamura, T., 1992. Preparation of Spinel-type Ferrite Thin Films by the Dip-coating Process and their Magnetic Properties. *Journal of Materials Science*. Volume 27, pp. 3645–3650
- Wang, J., Deng, T., Dai, Y., 2005. A New Kind of Dispersion—Colloidal Emulsion Aphrons. *Colloids and Surfaces A: Physicochemical and Engineering Aspects*, Volume 266(1-3), pp. 97–105
- Yang, J.S., Chang, C.R., 1994. Magnetization Curling in Elongated Hetero Structure Particles. *Phys. Rev.*, Volume 49(17), pp. 11877–11885